Mn Incorporation in Large Benthic Foraminifera: Differences Between Species and the Impact of pCO$_2$

Inge van Dijk[1,2]*, Lennart J. de Nooijer[2], Christine Barras[1] and Gert-Jan Reichart[2,3]

[1]UMR 6112 LPG-BIAF, Université d'Angers, Université de Nantes, CNRS, Angers, France, [2]Department of Ocean Systems, NIOZ-Royal Netherlands Institute for Sea Research and Utrecht University, Den Burg, Netherlands, [3]Faculty of Geosciences, Utrecht University, Utrecht, Netherlands

Element concentrations of calcite precipitated by foraminifera reflect chemical and physical properties of seawater and can therefore be used to reconstruct (paleo-)environmental conditions. Foraminiferal carbonate associated manganese incorporation (expressed here as Mn/Ca) is a potential proxy for seawater oxygenation, although the impacts of other environmental parameters need to be quantified before Mn/Ca can be robustly applied. Here we report the isolated impact of seawater carbonate chemistry on manganese incorporation in the shells of two large symbiont-bearing benthic foraminiferal species. Moreover, we investigated the role of biomineralization on manganese incorporation by using species with contrasting calcification pathways: the hyaline species *Amphistegina gibbosa* and the porcelaneous species *Sorites marginalis*. Furthermore, analyzing shells from a wide range of species grown under identical conditions allowed assessment of species-specific Mn incorporation in other foraminiferal species. Our observations show that species specific differences in biomineralization strategies are the dominant factor determining Mn content. Shells from porcelaneous species, with relatively high Mg contents, are generally also enriched in Mn compared to low-Mg/Ca foraminifera. Superimposed on the effect of biomineralization, chemical speciation of elements in seawater as a function of pCO$_2$ also affects their incorporation. Whereas the impact of the carbonate system is limited, the inter-specific differences call for species specific calibrations in order to use Mn uptake as a (paleo-)oxygenation proxy.

Keywords: foraminifera, manganese, carbon chemistry, pCO$_2$, proxy development

INTRODUCTION

The chemical composition of foraminiferal shells is widely used by paleoceanographers to reconstruct ocean conditions, because past fluctuations in physico-chemical conditions of seawater are recorded in the chemistry of the shell. For example, the Mg–Ca ratio (Mg/Ca) of foraminiferal calcite reflects seawater temperature (Nürnberg et al., 1996) and can hence be applied to fossil foraminifera to reconstruct past bottom water (Lear et al., 2000) and sea surface (Barker et al., 2005) temperatures. The toolbox that foraminiferal calcite provides, is ever expanding by addition of new elements of interest, including e.g., the recently proposed Sr/Ca (Keul et al., 2017) and S/Ca (Van Dijk et al., 2017a) as recorders of the seawater carbonate system. In addition, redox sensitive trace metals may serve as proxies to reconstruct (paleo-)oxygenation, a parameter for which accurate reconstruction methods are currently lacking. Manganese (Mn) is a promising candidate for

such a proxy, since solubility and/or the oxidation state of Mn is a function of the redox status of the environment (Tribovillard et al., 2006) and pore water carbonate chemistry (Middelburg et al., 1987). Manganese precipitates as a solid phase Mn oxyhydroxide under oxygenated conditions, but at lower oxygen levels, Mn oxyhydroxide is reduced and Mn^{2+} is released into the surrounding seawater. At high carbonate concentrations in the pore water, Mn^{2+} is removed by precipitation of Mn carbonate (rhodochrosite). Foraminifera incorporate dissolved Mn^{2+} (Reichart et al., 2003; Koho et al., 2015; Barras et al., 2018) and therefore the Mn/Ca of their shell is suggested to change with oxygenation conditions (Groeneveld and Filipsson, 2013; Koho et al., 2015; McKay et al., 2015; Ní Fhlaithearta et al., 2018). To further develop this proxy, it is necessary to i) investigate potential other (environmental) parameters influencing Mn incorporation and ii) obtain species-specific calibrations by culture or field studies, and ultimately iii) understand the incorporation pathways of Mn during biomineralization.

The influence of the carbonate system (e.g., pH, alkalinity, dissolved inorganic carbon) on foraminiferal Mn/Ca has, to our knowledge, not yet been studied. In theory, the carbonate system might have an effect on the Mn/Ca of foraminifera, since it is hypothesized that absorption layers might be involved in the incorporation of Mn (Barras et al., 2018) and adsorption on inorganically precipitated calcite depends on pH (Zachara et al., 1991). At higher pH, adsorption of Mn^{2+} might increase, which would result in overall higher foraminiferal Mn/Ca values. For the small benthic foraminifers *Ammonia* sp. and *Bulimina marginata*, thin bands with high Mn/Ca are observed at the start of calcite lamellae (Van Dijk et al., 2019b), which could be due to absorption layers that are exposed to the surrounding seawater between chamber formation events, as hypothesized in Barras et al. (2018). These high Mn/Ca layers are co-located with high Mg/Ca banding and are associated with a carbonate-associated species of Mn (Van Dijk et al., 2019b). Other processes related to seawater carbonate chemistry could also impact element incorporation (Ries et al., 2009). In inorganic calcite, precipitation rate controls incorporation of elements (Mucci, 1987). For Mn, a decreasing precipitation rate increases Mn partitioning ($D_{Mn} = Mn/Ca_{CALCITE}/Mn/Ca_{SEAWATER}$) and thus favors incorporation of Mn (Lorens, 1981). This is in contrast to Mg and Sr partitioning, which increases with calcite growth rate (Mavromatis et al., 2013). Consequently, when calcite precipitation rates in foraminifera are affected by e.g., ocean acidification or inorganic carbon chemistry in general, the effect on Mn- and Mg-incorporation is expected to be reversed. Unfortunately, so far the response of foraminifera to e.g., ocean acidification seems to be species-specific (Keul et al., 2013; Doo et al., 2014) making it difficult to predict overall effect of acidification on element incorporation.

As with other elements, Mn incorporation may well be species-specific, which would require calibration of this proxy for different species (e.g., see summary in Toyofuku et al., 2011). Barras et al. (2018) found that the two benthic species *Ammonia tepida* and *Bulimina marginata*, cultured under the same conditions, have a Mn partitioning of 0.08 and 0.6,

respectively, an offset of one order of magnitude. Incorporation of Mn appears to be coupled to that of Mg (Van Dijk et al., 2019b), similar to what is observed for other elements (Van Dijk et al., 2017b), possibly due to crystal lattice strain (Mucci and Morse, 1983; Evans et al., 2015) or simultaneous uptake (Van Dijk et al., 2019a). Even if the relative sensitivity of Mn/Ca to oxygenation is the same for different species, as suggested for certain proxies (e.g., S/Ca; Van Dijk et al., 2017a), the absolute Mn/Ca value is still needed for reconstruction of oxygenation. Therefore, Mn/Ca values of both hyaline and porcelaneous species have to be known before application of this potential oxygenation proxy.

However, there is no consensus on key processes involved in foraminiferal calcification (review in De Nooijer et al., 2014). Uptake of ions could occur for instance through seawater endocytosis (seawater vacuolization model; Erez, 2003; Bentov et al., 2009) or transmembrane transport (Nehrke et al., 2013; Mewes et al., 2015), and is either precipitated from a closed reservoir (Elderfield et al., 1996; Evans et al., 2018) or by a continuous ion supply where precipitation follows a classical or a non-classical pathway (Jacob et al., 2017). These models do not specify how Mn is taken up from seawater by the organism and how it is subsequently incorporated into foraminiferal calcite. According to the seawater vacuolization model model, Mn is transported in a seawater-filled vacuole to the site of calcification (SOC). Whether Mn is actively removed, like is hypothesized for Mg (Bentov and Erez, 2006), remains to be investigated. In the transmembrane transport model, Ca is transported through transmembrane channels, which may occasionally transport other cations with a radius close to the Ca^{2+}, like Zn^{2+} and Cd^{2+} (Gonçalves et al., 1999). This would also be the case for Mn^{2+} ions, since the ionic radius of Mn^{2+} (0.8 Å) is similar to that of Ca^{2+}(1.0 Å). Based on culture evidence, Barras et al. (2018) hypothesize that the incorporated Mn in the foraminiferal shell might be partly related to an organismal calcification pathway (biological incorporation), as discussed above, in combination with an inorganic pathway (abiological incorporation). This inorganic pathway involves adsorption of Mn ions on specific sites on the exposed outer surface of the calcite shells (Mucci and Morse, 1983) in between chamber formation events. Clearly, further research is needed to understand Mn pathways and create a fundamental basis to explain the empirical relation between foraminifera Mn and the concentration of dissolved oxygen and seawater [Mn].

In this study we address the major issues mentioned above by investigating the effect of seawater carbonate chemistry on shell Mn/Ca values. Observations are used to evaluate the proposed possible pathways of Mn during foraminiferal calcification. We investigated single-chamber Mn/Ca values from a controlled culture experiment with two larger benthic species of foraminifera, *Amphistegina gibbosa* hosting diatom symbionts (Lee et al., 1995), which precipitates a hyaline shell with intermediate Mg/Ca (~2% wt Mg) and porcelaneous species *Sorites marginalis*, which calcifies a shell with high Mg content (>4% wt Mg) and host dinoflagellates (Müller-Merz and Lee, 1976). Specimens were cultured in one of four different conditions, with a *p*CO₂ of 350, 450, 760, or 1,200 ppm, to

TABLE 1 | Carbon parameters of the culture media per pCO$_2$ set-point.

Treatment	Set-point	Measured	Calculated CO2SYS			
	pCO$_2$ (ppm)	TA (µmol/kg)	DIC (µmol/kg)	[CO$_3^{2-}$] (µmol/kg)	pH (total scale)	Ω_{CALCITE}
A	350	2,302.8 ± 8.2	2,007.5 ± 10.7	220.7	8.06	5.4
B	450	2,305.2 ± 5.8	2,021.3 ± 12.5	200.0	8.01	4.9
C	760	2,304.4 ± 0.9	2,100.8 ± 13.4	153.7	7.87	3.7
D	1,200	2,300.3 ± 0.7	2,201.4 ± 4.1	92.2	7.61	2.2

Total alkalinity (TA) and dissolved inorganic carbon (DIC) have been measured directly, the other carbon parameters are calculated with CO2SYS. For details see van Dijk et al. (2017).

study the effect of the carbonate system on the incorporation of Mn in foraminiferal calcite. In addition, we analyzed a wide range of species sampled from an Indo-Pacific coral reef aquarium (Ernst et al., 2011) to study species-specific partitioning in hyaline and porcelaneous larger benthic foraminifera from a controlled environment.

METHODS

Foraminiferal Samples

In this study we analyzed specimens of two species of foraminifera, *A. gibbosa* and *S. marginalis* grown under a range of controlled pCO$_2$, as well as larger benthic foraminifera collected from an Indo-Pacific reef aquarium. The experimental design of the culture experiment under different pCO$_2$ has been described in detail in Van Dijk et al. (2017b). In short, different species of larger benthic foraminifera collected in the Caribbean Sea were incubated under controlled conditions at the Caribbean Netherlands Science Institute (CNSI; St. Eustatius). Foraminifera were cultured in groups in 70 ml Falcon® tissue bottles in four batches of seawater with added Calcein (5 mg/l), which were in equilibrium with four different pCO$_2$ (350, 450, 760, and 1,200 ppm named, respectively, treatment A, B, C, and D) by a pCO$_2$-control system developed in-house (described in detail in Webb et al., 2017). Culture media was replaced every 4 days. At the start and termination of the experiment, 125 ml samples from the stock seawater solutions (one for each experimental treatment) were collected to analyze the concentration of dissolved inorganic carbon and total alkalinity on a Versatile INstrument for the Determination of Titration Alkalinity at the CNSI. Physico-chemical parameters of the culture conditions can be found in **Table 1**. Foraminifera were cultured at 25 ± 0.2°C for 21 days, during which they build on average 2.4 and 5.0 chambers for *A. gibbosa* and *S. marginalis*, respectively. After termination of the experiment, specimens were rinsed three times with de-ionized water and dried at 40°C. Foraminiferal samples were transported in slides to the Royal Netherlands Institute for Sea Research (NIOZ) to investigate the Mn/Ca of the shell and growth parameters. To assess the number of chambers added during the experiment, fluorescent calcein-stained chambers were counted using a ZEISS Axioplan 2 fluorescence microscope equipped with appropriate excitation and emission optics. Pictures were taken using a ZEISS Axiocam MRc 5 camera.

At Burgers' Zoo in Arnhem, Netherlands, coral debris, rich in foraminifera (Ernst et al., 2011) were collected from the Indo-Pacific coral reef aquarium, one of the largest coral reef aquaria in the world. From these coral debris, hyaline (*Amphistegina lessonii* and *Heterostegina depressa*) and porcelaneous (*Sorites orbiculus*, *Spiroculina angulata*, *Spiroculina communis*, *Quinqueloculina pseudoreticulata*, *Quinqueloculina* sp.) species of foraminifera were isolated to analyze the shell chemistry. Foraminifera from both the experiment and the aquarium were cleaned following an adapted version of the Barker protocol (Barker et al., 2003), described in Van Dijk et al. (2017a, 2017b). In short, foraminifera were cleaned using an oxidizing step in which organics were removed with a 1% H$_2$O$_2$ solution (buffered with 0.1 M NH$_4$OH), and consequently, after gentle ultrasonication, rinsed with ultrapure water and dried in a laminar flow cabinet.

Foraminiferal Carbonate Analyses
Laser Ablation-Inductively Coupled Plasma Mass Spectrometry

Elemental composition of individual fluorescent chambers of cultured specimens was analyzed by laser ablation-inductively coupled plasma mass spectrometry (ICP-MS) (Reichart et al., 2003; Van Dijk et al., 2017b). In short, the laser system comprising of an ArF Excimer laser (Existar) with deep UV 193 nm wavelength and <4 ns pulse duration (NWR193UC, New Wave Research) was equipped with a Two Volume 2 cell (New Wave Research), characterized by a wash-out time of 1.8 s (1% level). Single chambers were ablated in a helium environment using a circular laser spot with a diameter of 80 µm (*S. marginalis*) and 60 µm (*A. gibbosa*). Foraminifera were previously analyzed (Van Dijk et al., 2017b), but at that time Mn could not be included as an analyte due to interferences with ArN due to the addition of N$_2$ to obtain better counting statistics for e.g., Na. Whenever possible, we re-ablated all calcein-stained chambers one to three times. All foraminiferal samples were ablated with an energy density of 1.0 ± 0.1 J/cm^2 and a repetition rate of 6 Hz. The resulting aerosol was transported with a helium/argon flow to the quadrupole ICP-MS (iCAP Q, Thermo Scientific). Other monitored masses included ^{7}Li, ^{23}Na, ^{24}Mg, ^{25}Mg, ^{27}Al, ^{43}Ca, ^{44}Ca, ^{55}Mn, ^{88}Sr, and ^{137}Ba.

At the start of each series we analyzed several carbonate standards, including JCt-1 (coral carbonate) and two in-house standards, namely NFHS (NIOZ Foraminifera House Standard; Mezger et al., 2016) as well as an Iceland spar NCHS (NIOZ Calcite House Standard). At the end of each series we analyzed SRM NIST612 and NIST610 glass standard in triplicate (using an energy density of 5.0 ± 0.1 J/cm^2). We further analyzed JCp-1 (coral, *Porites* sp.; Okai et al., 2002) and MACS-3 (synthetic

Treatment	A	B	C	D
pCO$_2$ (ppm)	350	450	760	1,200
A. gibbosa	11(25)	28(74)	21(51)	15(43)
S. marginalis	10(33)	7(21)	14(42)	18(54)

calcium carbonate) at the start of each series, and to monitor drift after every ten samples. All element to calcium ratios were calculated with an adapted version of the MATLAB based program Signal Integration for Laboratory Laser Systems (Guillong et al., 2008). Signal Integration for Laboratory Laser Systems was modified by NIOZ to evaluate LA-ICP-MS measurements on foraminifera, allowing import of Thermo Qtegra software sample list, laser data reduction and laser LOG files (as described in Mezger et al., 2016; Van Dijk et al., 2017b). Some major adaptions include improved automated integration and evaluation of (calibration and monitor) standards, quality control report of the monitor standards and export in element to calcium ratios (mmol/mol). Integration profiles were manually selected for evaluation, by e.g., monitoring decrease in Ca counts and the Al signal, which can be used as a sign of potential contamination or diagenesis of the outer or inner layer of calcite. Calibration was performed against the MACS-3 carbonate standard, with ^{43}Ca as an internal standard and the multiple measurements of MACS-3 were used to apply a linear drift correction. Relative analytical precision, expressed as the relative standard deviation (RSD) of all MACS-3 analyses, is 3% for ^{7}Li/Ca, 3% ^{23}Na/Ca, 3% for ^{24}Mg/Ca, 3% for ^{25}Mg/Ca, 2% for ^{55}Mn/Ca, 3% for ^{88}Sr/Ca, and 3% for ^{137}Ba/Ca. Accuracy, based on values for JCp-1 standardized to MACS-3, was 95 and 93% for Mg/Ca and Mn/Ca, respectively.

In total, 193 and 150 analyses were performed on *A. gibbosa* and *S. marginalis*, respectively (see **Supplementary Material Data Sheet**). For details on the amount of specimens and analysis per species, see **Table 2**. We removed outliers, 13 in total, from the database based on 1.5 × interquartile range of Mn/Ca. Furthermore, we calculated the average Mn/Ca and Mg/Ca per species per treatment and partition coefficient between seawater and foraminiferal calcite, D, which is expressed as D_E = (E/Ca$_{CALCITE}$)/(E/Ca$_{SW}$), in which E is the element of interest. Since these foraminifera were previously analyzed, we also compare our new data with the Mg/Ca data of a previous study (Van Dijk et al., 2017b).

Sector Field-Inductively Coupled Plasma Mass Spectrometry

Foraminifera from Burgers' Zoo were grouped per species (*A. lessonii*, *Heterostegina depressa*, *Sorites orbiculus*, *Spiroculina angulate*, *Spiroloculina communis*, *Quinqeloculina pseudoreticulata*, and *Quinqeloculina* sp.) and dissolved in 0.5 ml 0.1 M HNO$_3$. A 5 s pre-scan for ^{43}Ca was performed on an Element 2 sector field double focusing mass spectrometer (SF-ICP-MS) to determine the [Ca] in the dissolved foraminiferal

calcite solutions. According to these results, samples were diluted to 100 ppm Ca. Elemental composition of the foraminifera was measured for a wide range of isotopes, including ^{24}Mg, ^{55}Mn, ^{43}Ca at medium resolution with a 300 ml/min flowrate using a peristaltic pump. Samples were measured against six ratio calibration standards with similar matrix. In addition to the foraminiferal samples, we measured several standards to monitor drift and the quality of the analyses, including NFHS (NIOZ Foraminifera House Standard; for details see Mezger et al., 2016), JCt-1 (Giant Clam, *Tridacna gigas*) and JCp-1 (coral, *Porites* sp.; Okai et al., 2002). One of the ratio calibration standards was measured after every fifth sample to monitor drift. Accuracy of Mg/Ca is 105 and 101% for JCt-1 and JCp-1, respectively, with an external precision of 0.4% for both standards. For Mn/Ca, only MACS-3 has a certified value, and accuracy of our measurements is 101% when using this standard.

Seawater Measurements

The sampling strategy and general seawater composition (Ca, Mg, Na, Sr and Ba) of the media used in the pCO$_2$ controlled experiment has been described in Van Dijk et al. (2017b). In short, at the start and end of the experiment and during replacement of the culture media every four days, subsamples were collected and acidified with three times Quartz distilled HCl to pH ~ 1.8. Additionally, seawater from the aquarium in Burgers' Zoo was sampled during collection of coral debris at two different occasions. In total, we collected three seawater samples (total n = 6) in 50 ml Falcon tubes, which were returned to the laboratory, acidified and stored at 7°C upon analysis. The seawater composition of the experimental samples as well as the Burgers' Zoo seawater was analyzed on an Element-2 SF-ICP-MS run in medium resolution mode. International Association for the Physical Sciences of the Ocean Standard Seawater was used as a drift monitor. Analytical precision (RSD) was 3% for Ca, 4% for Mg, 1% Na, 1% for Sr and 5% Ba. For the samples of the culture experiment, we obtained average values of 5.25 ± 0.06 mol/mol for Mg/Ca, 44.6 ± 0.6 mol/mol for Na/Ca, 8.63 ± 0.05 mmol/mol for Sr/Ca, and 9.04 ± 0.47 µmol/mol for Ba/Ca. For Burgers' Zoo seawater, Mg/Ca was 6.1 ± 0.9 mol/mol.

Due to the low concentration, [Mn] of subsamples from the culture experiment and tropical aquarium had to be analyzed using a commercially available pre-concentration system, SeaFAST S2. With the SeaFAST system elements with low concentrations are pre-concentrated to values above detection limit of the SF-ICP-MS. Accordingly, we measured Cd, Pb, U, B, Ti, Mn, Fe, Co, Ni, Cu, and Zn. In short, 10 ml of sample was mixed with an ammonium acetate buffer to pH 6.2 and loaded on a column containing NOBIAS chelating agent. After rinsing the column with a diluted ammonium acetate buffer the metals were eluted in 750 µL of quartz distilled 1.5 M HNO$_3$ before being quantified on the SF-ICP-MS. Analytical precision (RSD) was 4% for Mn and we obtained an average seawater Mn/Ca value of 5.4 ± 0.3 µmol/mol for the culture experiment, and of 14.8 ± 0.2 µmol/mol for the Burgers' Zoo samples.

FIGURE 1 | Average foraminiferal Mn/Ca with standard deviation and boxplot of all datapoints per treatment A, B, C, and D for *A. gibbosa* (**A**; circles) and *Sorites marginalis* (**B**; diamonds). Insets show SEM images of both species with laser ablation spots visible. Scale bar = 500 µm. Average Mn/Ca ± standard error (gray bar) vs. pCO$_2$, with regression line and 95% confidence interval (gray area) for *A. gibbosa* (**C**; Mn/Ca = 0.003 × pCO$_2$ +2.44 with R^2 = 0.95 and p < 0.0025) and *S. marginalis* (**D**; Mn/Ca = 0.05 × pCO$_2$ + 32.4 with R^2 = 0.91 and p < 0.01).

RESULTS

Foraminiferal Mn/Ca and Mg/Ca vs. pCO$_2$ From Controlled Experiments

For the hyaline species *A. gibbosa*, Mn/Ca is 4.4 ± 2.1 µmol/mol for all measurements on average. When pCO$_2$ increases from 350 to 1,200 ppm, average Mn/Ca increase significantly (p < 0.0025; R^2 = 0.95) with pCO$_2$ (**Figure 1C**). From lowest to highest pCO$_2$ condition, Mn/Ca increases from 3.2 to 5.9 µmol/ mol (**Figure 1A**), an overall increase of factor 1.9, or 22% per 100 ppm CO$_2$. For the correlation between [CO$_3^{2-}$] and pH with Mn/Ca, see **Supplementary Figure S1**. Mn/Ca of the porcelaneous species *S. marginalis* are ~11 times higher than the hyaline species *A. gibbosa*. For this species, Mn/Ca increases significantly with pCO$_2$ as well (p < 0.01; R^2 = 0.91; **Figure 1D**) by a factor of 2.1, or 25% per 100 ppm

CO$_2$, from 42.7 to 90.3 µmol/mol. For both species, standard deviation (SD) per treatment increases with increasing pCO$_2$, and hence increasing Mn/Ca. For *A. lessonii*, the relative SD (RSD) is on average 40% for the different conditions, while for *S. marginalis*, the RSD increases from 35 to 51% with increasing pCO$_2$.

Individual measurements of Mn/Ca and Mg/Ca for both species are shown in **Figure 2**. Average Mg/Ca is 27.4 ± 5.3 and 141.9 ± 5.3 mmol/mol for *A. gibbosa* and *S. marginalis*, respectively (**Table 3**), which fits very well with earlier measurements on the same specimens, where the average Mg/ Ca values obtained were 27.7 and 145.8 mmol/mol, respectively (Van Dijk et al., 2017b), illustrating the good reproducibility of the LA-ICP-MS analyses. Partitioning of Mg and Mn is, on average respectively 4.7 and 13.5 times higher in *S. marginalis* compared to *A. gibbosa*.

Figure 2 | Mn/Ca vs. Mg/Ca of individual laser ablation measurements for *A. gibbosa* **(A)** and *S. marginalis* **(B)**. For *A. gibbosa*, Mn/Ca increases with Mg/Ca following Mn/Ca = 0.17 × Mg/Ca-0.23.
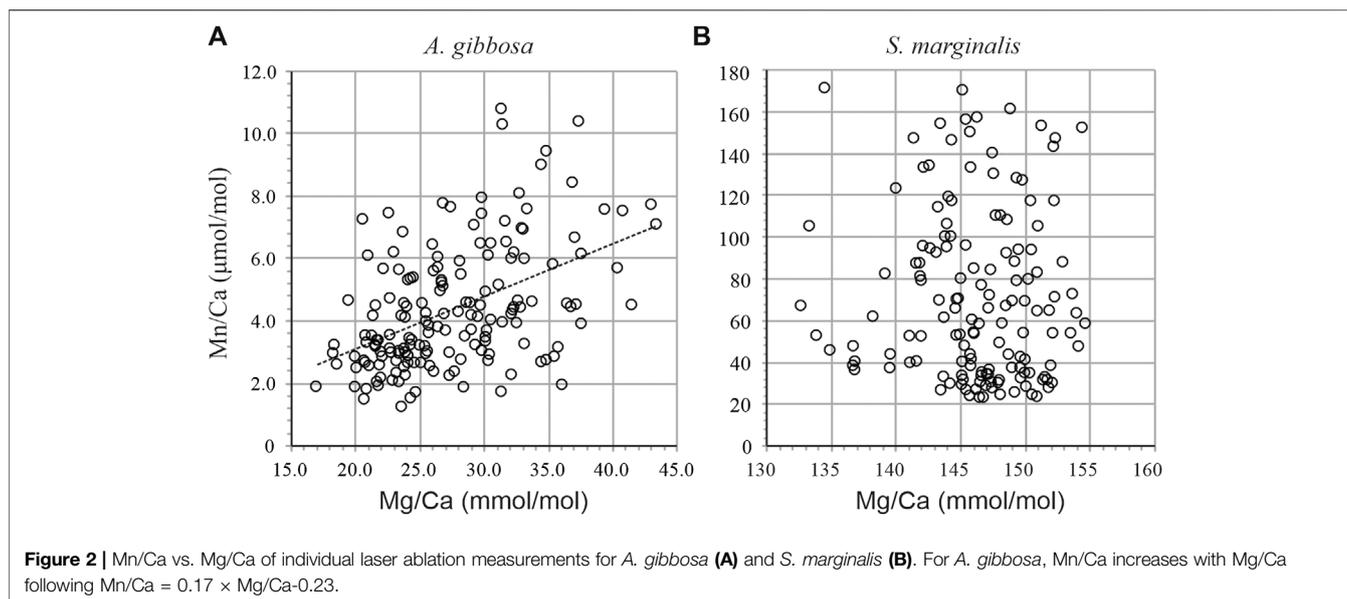
TABLE 3 | Mn/Ca and Mg/Ca [±standard deviation (SD)] and element partitioning with propagating SD of hyaline species *Amphistegina gibbosa* and porcelaneous species *Sorites marginalis* cultured at different *p*CO₂.

Species	pCO₂ (ppm)	Mn/Ca (µmol/mol ± SD)	D_{Mn}	Mg/Ca (mmol/mol ± SD)	D_{Mg} × 1,000
Amphistegina gibbosa	350	3.0 ± 1.2	0.55 ± 0.22	27.8 ± 4.6	5.3 ± 0.9
	450	4.0 ± 1.6	0.73 ± 0.29	25.3 ± 5.4	4.8 ± 1.1
	760	4.8 ± 2.2	0.89 ± 0.40	30.5 ± 4.5	5.7 ± 0.8
	1,200	5.6 ± 1.9	1.03 ± 0.35	27.6 ± 4.7	5.2 ± 0.9
Sorites marginalis	350	42.7 ± 14.9	7.9 ± 2.7	142.6 ± 5.3	27.2 ± 1.0
	450	61.7 ± 27.4	11.3 ± 5.0	148.1 ± 3.3	28.2 ± 0.6
	760	71.9 ± 35.0	13.2 ± 6.4	147.9 ± 3.4	28.2 ± 0.6
	1,200	90.3 ± 46.2	16.6 ± 8.5	146.2 ± 4.4	27.8 ± 0.8

Foraminiferal Growth as a Function of pCO₂ From Controlled Experiments

On average for all conditions, ~80% of the specimens of *S. marginalis* (for example, see **Figure 3B**) added new chambers during the experiment, vs. ~90% of *A. gibbosa* individuals (for example, see **Figure 3C**). There is no significant trend of chamber addition rate (number of chambers added per day) with pCO₂ for both species studied (**Figure 3A**). On average, specimens of *S. marginalis* added more than two times as many chambers during the culture period, 0.28 ± 0.12 chamber per day vs. 0.12 ± 0.05 for specimens of *A. gibbosa*.

Mn and Mg Partitioning of Foraminifera From the Indo-Pacific Aquarium

On average partitioning of Mn (D_{Mn}) and Mg (D_{Mg} × 10³) are, respectively: 0.8 ± 0.4 and 5.5 ± 0.1 for *A. lessonii*, 1.9 ± 0.8 and 26.7 ± 0.3 for *H. depressa*, which are both hyaline species; and 16.2 ± 3.2 and 26.7 ± 0.4 for *S. orbiculus*, 11.8 ± 1.6 and 25.3 ± 0.4 for *S. angulata*, 18.6 ± 1.9 and 22.5 ± 0.4 for *S. communis*, 23.0 ± 1.8 and 25.9 ± 0.4 for *Q. pseudoreticulata* and 20.4 ± 2.7 and

23.5 ± 0.4 for *Quinqueloculina* sp., which are five porcelaneous species (see **Table 4**). The D_{Mn} and D_{Mg} values are plotted together to visualize possible trends between the two groups of foraminifera (**Figure 4**). In general, porcelaneous species incorporate more Mn than hyaline species and the species investigated have similar Mg content (D_{Mg} × 10³ of 22.5–26.7). In contrast, hyaline species comprise a wider range in D_{Mg} compared to the porcelaneous species.

DISCUSSION

Mn Incorporation as a Function of pCO₂

For both species studied here, the hyaline *A. gibbosa* and the porcelaneous *S. marginalis*, we observe that shell Mn/Ca increases with increasing pCO₂ (and hence decreasing sea water pH, [CO₃²⁻] or Ω). A similar trend was observed for the same species for Zn and Ba, but was not found case for elements such as Mg, Na and Sr (Van Dijk et al., 2017b). We do not suggest that Mn/Ca values can be used as recorders of the carbonate system, since Mn/Ca in foraminiferal shells is hypothesized

FIGURE 3 | Average chamber addition rates **(A)** per day (±SD) of *S. marginalis* (blue diamonds) in blue and *A. gibbosa* (red circles). Right panels show pictures of *S. marginalis* **(B)** and *A. gibbosa* **(C)**.
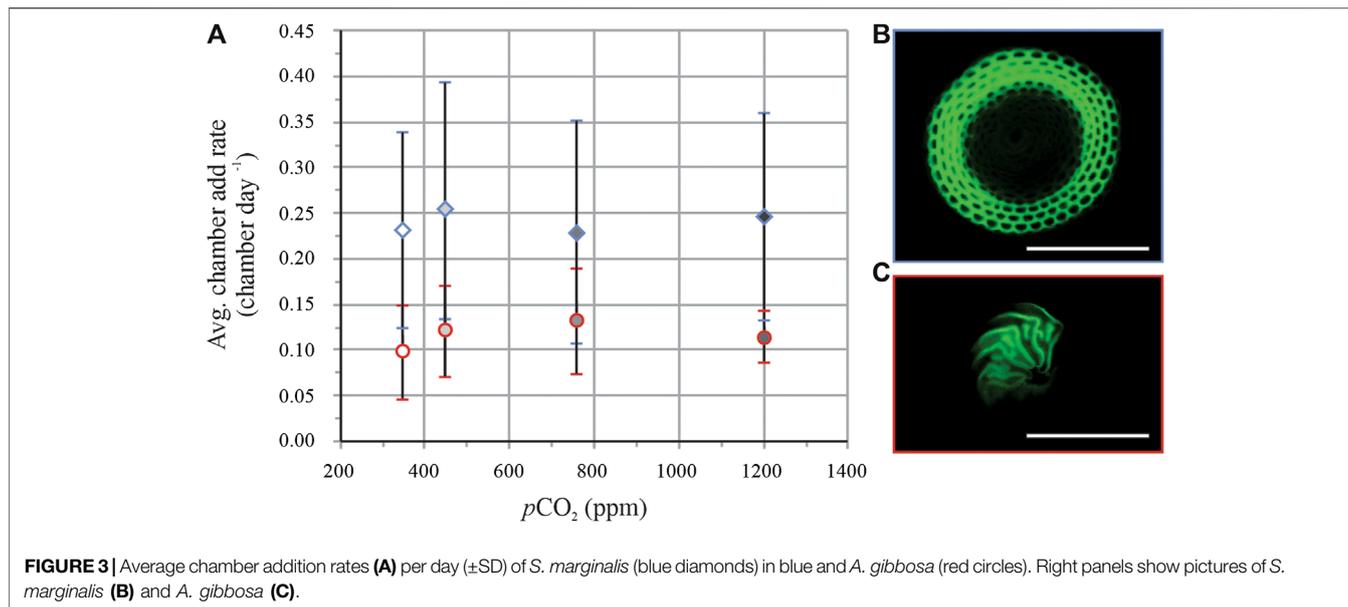
influenced by seawater [Mn] (Barras et al., 2018), but this could hamper the precision of this proxy (cf. Chapter 4.3). Still, comparing sensitivity of Mn incorporation to pCO$_2$ to that of other elements provides information on the underlying mechanisms involved in organismal trace element uptake. Even though the slope of the Mn/Ca-pCO$_2$ calibrations differs between species (0.003 for *A. gibbosa* and 0.05 for *S. marginalis*), the incorporation of Mn as a function of pCO$_2$ is, in terms of relative sensitivity, similar for *A. gibbosa* (22% increase in Mn/Ca per 100 ppm CO$_2$) and *S. marginalis* (25% increase in Mn/Ca per 100 ppm increase in CO$_2$). This is surprising since these species are known to have contrasting calcification strategies (e.g., Bé et al., 1979; De Nooijer et al., 2009a; Hemleben et al., 1986). This could imply that Mn incorporation as a function of pCO$_2$ is governed by identical processes in calcification. This might relate to the (active) uptake of trace elements or the subsequent precipitation of carbonate. The first factor inherently includes e.g., symbiont and enzyme activity, speciation of Mn in seawater and pH-dependent absorption of Mn to calcite. The second factor, actual carbonate precipitation, includes both abiotic

factors such as precipitation rate and also potentially biological controls during this phase.

Impact of pCO$_2$ on Biological Processes

Growth of marine organisms is, in general, negatively impacted by current changes in oceanic conditions, global warming and ocean acidification (e.g., Orr et al., 2005; Kroeker et al., 2013). For inorganic precipitation experiments, crystal growth rate has a negative effect on incorporation of Mn, resulting in lower Mn/Ca values at higher precipitation rates (Lorens, 1981). Therefore, an increase in Mn incorporation in foraminiferal calcite with pCO$_2$ might be explained by a decrease in the precipitation rate of the foraminiferal shell at higher pCO$_2$, assuming that results from

TABLE 4 | Mn and Mg partitioning with propagating standard deviation for species collected from Burgers' Zoo aquarium.

Species	D_{Mn}	$D_{Mg} \times 10^3$
Hyaline species		
Amphistegina lessonii	0.8 ± 0.4	5.5 ± 0.1
Heterostegina depressa	1.9 ± 0.8	26.7 ± 0.3
Porcelaneous species		
Sorites orbitolis	16.2 ± 3.2	26.7 ± 0.4
Spiroculina angulata	11.8 ± 1.6	25.3 ± 0.4
Spiroculina communis	18.6 ± 1.9	22.5 ± 0.4
Quinqueloculina pseudoreticulata	23.0 ± 1.8	25.9 ± 0.4
Quinqueloculina sp.	20.4 ± 2.7	23.5 ± 0.4

FIGURE 4 | Overview of the average partitioning of Mn (D_{Mn}) as a function of $D_{Mg} \times 10^3$ for foraminiferal species studied here, from both the controlled pCO$_2$ experiment (average value, closed symbols) and the Indo-Pacific coral reef aquarium (open symbols). Hyaline species and porcelaneous species are indicated with circles and diamond respectively. Error bars indicate SD and numbers indicate species.

synthetic calcites can be directly translated to biogenic calcite. In our experiments, we measured the average number of newly formed chambers per day for both species and we can conclude that pCO$_2$ concentrations have no impact on their calcification capacity, i.e., chamber addition rates (n chambers day^{-1}) are stable over the range of culture conditions investigated. However, from these data, we cannot evaluate the calcite precipitation rate itself. As shown by meta-studies on the effect of pCO$_2$ on foraminiferal calcification rates, calculated using a variety of methods by Doo et al. (2014) and Keul et al. (2013), response of foraminifera growth is very species-specific, including negative, positive and no effect growth parameters with increasing pCO$_2$ conditions. Studies that investigate calcification rates of similar species as used in this study in more detail, i.e., by calculating changes in surface area and buoyant weight or shell density as a function of pH, observed opposite trends according to the species considered: no decrease in growth rates for dinoflagellate-bearing porcelaneous species like *Marginopora vertebralis* after extended periods (30–43 days) at a pH 7.6–7.4 (Vogel and Uthicke, 2012; Prazeres et al., 2015), while the diatom-bearing *A. lessonii* showed a steady reduction of shell density and volume at lower pH (Prazeres et al., 2015). Assuming that the calculated calcification rates in these studies would be correlated to crystal growth rates, there would be no change in precipitation rate in porcelaneous species in the range of pH studied here and therefore the trend in Mn/Ca would not be explained by precipitation rate. However, the link between calcite addition rate and crystal growth rate still needs to be explored. A detailed study on foraminiferal calcification rate, in which chamber addition rates should be clearly decoupled from crystal growth rates, is necessary to evaluate the impact of precipitation rate on foraminiferal Mn/Ca values and other elemental ratios in general. Since we cannot prove that the observed trends in Mn/Ca are (only) driven by carbonate chemistry-drive changes in crystal growth rates, we also explore other possibilities.

Foraminiferal Mn/Ca values may be link to Ca-ATPase, which appears to play an important role in regulating Ca^{2+} uptake for calcification (Toyofuku et al., 2017). According to Prazeres et al. (2015), upregulation of Ca-ATPase is confirmed at lower pH values for *A. lessonii*. Their interpretation is that the enzyme is used for removing Ca^{2+} out of the SOC due to shell dissolution. However, this is not logical due to the large amount of Ca^{2+} foraminifera need for calcification (De Nooijer et al., 2009a); even if shell dissolution would lead to an increase in Ca^{2+} in the SOC (and not the surrounding seawater), this resource is much too valuable to transport outwards. We therefore argue that Ca-ATPase is used in foraminiferal calcification to take up Ca^{2+}, as proposed by Toyofuku et al. (2017). Higher activity of this enzyme might also increase the accidental uptake of Mn^{2+}, due to the similarity in ionic radii of Mn^{2+} and Ca^{2+}. This would in theory lead to higher Mn availability in the SOC and therefore incorporation in the shell at lower pH and higher pCO$_2$. However, this increase in Ca-ATPase activity is not observed for porcelaneous species like *S. marginalis*, in which we also observe a positive correlation between pCO$_2$ and Mn/Ca values and can thus not explain the increase in Mn/Ca in this species.

Effect of pCO$_2$ on Speciation and Adsorption of Mn

Incorporation of Mn might be governed by the speciation of Mn in seawater with pCO$_2$. Besides Mn, the incorporation of Ba and Zn also increases with higher pCO$_2$, which could be explained by changes in the chemical speciation of these elements, induced by seawater carbonate chemistry (Van Dijk et al., 2017b; Van Dijk et al., 2017c). We have tested this hypothesis for Mn using the software package PHREEQC (v.2; Parkhurst and Appelo, 1999) and the standard PHREEQC llnl database, which allows modeling of bioavailability of different chemical species (eg, Mn^{2+}, MnCO$_3$) in seawater. The model shows a shift in element speciation with pCO$_2$ (**Figure 5A**). When seawater chemistry changes from low pCO$_2$ (or high pH) to higher pCO$_2$ (or low pH), we observe an increase in the activity of free Mn^{2+}, soluble carbonate-complexes decreases, which is similar to the findings for Zn and Ba speciation with pCO$_2$ (Van Dijk et al., 2017b).

When considering other pH/CO$_3$$^{2-}$ depending proxies, the increase in Mn over the studied range in pCO$_2$ is considerably smaller than for example the increase in Zn incorporation (Van Dijk et al., 2017b). For instance, when comparing the relative change in the activities of Mn and Zn (**Figure 5B**), the change in activity of free Zn (Zn^{2+}; 10%) is larger than the changes in free Mn (Mn^{2+}; 2%). This could then explain why Zn/Ca$_{CALCITE}$ is more sensitive to pCO$_2$ compared to Mn/Ca$_{CALCITE}$. For instance, for *A. gibbosa*, Mn/Ca increases 22% per 100 ppm CO$_2$ (this study; **Figure 1**), while Zn/Ca increases 53% (Van Dijk et al., 2017b), which might be due to the higher increase in availability of free ions of Zn compared to Mn (**Figure 5B**).

Based on the PHREEQC model, increase in Mn incorporation at higher pCO$_2$ could be explained by more (bio)available Mn^{2+} (**Figures 5C,D**) which may be transported by Ca-channels during calcification (Nehrke et al., 2013). However, to accurately model chemical speciation during chamber formation and assess its role in element incorporation, it is crucial to know the carbonate chemistry of both the foraminiferal microenvironment and at the SOC. In addition to the pH during calcification (De Nooijer et al., 2009; Toyofuku et al., 2017; Glas et al., 2012a) a second parameter of the inorganic carbon system is necessary to reconstruct the complete carbon system inside and outside the foraminifer. Since there are examples of functioning proxies for seawater carbonate chemistry, one of the most established one being the boron isotopic composition of foraminiferal shells as a proxy for seawater pH (e.g., Sanyal et al., 1996; Pagani et al., 2005; Foster and Rae, 2016), it is likely that the external and internal pH are in some way affected by ocean acidification.

Finally, Barras et al. (2018) suggested that Mn might be (partially) incorporated into the shell by incorporation into adsorption layers. This was hypothesized to explain different ontogenetic trends (differences in chamber to chamber values of Mn/Ca) observed between species of (deep-sea and intertidal) small benthic foraminifera. Sorption of divalent metals, like Mn^{2+}, on the surface of synthetic calcite is pH dependent (Zachara et al., 1991), with lower pH resulting in lower adsorption. If such adsorption process would exist in large tropical species, which has not been proven yet, we would have expected that higher pCO$_2$ would decrease Mn

FIGURE 5 | Modeled activity of Mn by PHREEQC. Speciation of free (Mn^{2+}; closed symbols) and complexed ($MnCO_3$; open symbols) Mn plotted as a function of pCO₂ **(A)**. Relative change in activity of free Mn^{2+} and Mn-CO₃ complexes **(B)** plotted together with relative activity changes of free Zn^{2+} (solid gray line) and $ZnCO_3$ complexes (dashed gray line) from van Dijk et al. (2017c). Mn partitioning for both species (*A. gibbosa* = red circles; *Sorites marginalis* = blue diamonds) as a function of Mn^{2+} activity **(C)** and $MnCO_3$ activity **(D)**, with symbol filling corresponding to pCO₂ of the treatments, in which darker filling represents higher pCO₂ conditions, see also **Figure 2**.

incorporation. However, we observe the exact opposite. Either the hypothesis of adsorption layers playing a role during biocalcification is not correct, at least for both large benthic species studied here, or this effect is much smaller and therefore negligible compared to e.g., changes in Mn speciation.

Manganese Incorporation in Different Species of Foraminifera

Since speciation of Mn is sensitive to carbonate chemistry of the seawater (**Figure 5A**) and also at the SOC, offsets in internal pH during calcification between species might be responsible for observed difference in Mn incorporation. Since internal (De Nooijer et al., 2009a) and external pH (Glas et al., 2012b) are linked due to proton pumping (Toyofuku et al., 2017), a higher internal pH would correspond to a lower pH in the foraminiferal microenvironment. This will lead in turn to a higher activity of free Mn outside the organism, which could be transported through Ca-channels. Following this hypothesis, foraminifera with higher Mn/Ca, like *H. depressa* (**Figure 4**), might have a higher passive transport of Mn and/or a higher internal pH during calcification compared to *A. gibbosa*. No independent evidence exists, however, for such a difference in internal pH between species or between the

groups precipitating a hyaline or porcelaneous shell. For example, for hyaline species, also changes in the regulation of Ca-ATPase (Prazeres et al., 2015) between species might be responsible for the observed differences in Mn incorporation.

When investigating Mn incorporation across a wider range of foraminiferal species, we observe that overall Mn/Ca values seem linked to Mg content which seems to primarily reflect calcification strategy (**Figure 4**). Porcelaneous species incorporate in general more Mn and Mg, however we observe no correlation between shell Mg/Ca and Mn/Ca within this group of species. In contrast, within the hyaline species, we observe that species that have a higher Mg content also incorporate more Mn. Based on inorganic precipitation experiments, higher precipitation rates would lead to higher Mg partitioning (Mavromatis et al., 2013), but would also lower Mn/Ca$_{CALCITE}$ due to a decrease in partitioning (Lorens, 1981). This could potentially explain the observed increase of Mg/Ca$_{CALCITE}$ and simultaneous decrease of Mn/Ca$_{CALCITE}$ with temperature in cultured *A. lessonii* (Van Dijk et al., 2019a). However, it does not explain the trends we observe for different hyaline and porcelaneous species (**Figure 4**), in which both Mg/Ca and Mn/Ca increase in concert. Whatever the cause of the offset in Mg content between species (discussed in more detail in Van Dijk et al., 2019a), difference in Mg/Ca can potentially by itself alter the

incorporation of other elements, through crystal lattice distortion. Based on inorganic experiments, Mg incorporation alters the structure of the crystal lattice (Mucci, 1987) and the resulting strain on the destabilized crystal lattice allows for higher incorporation of other trace metals. Lattice distortion has been proposed before to explain an increase in Na with Mg for larger benthic foraminifera (e.g., Evans et al., 2015). Similarly, this might explain the observed trends for hyaline species, for which we observe a co-variation of Mn/Ca and Mg/Ca between individuals (**Figure 2**) and between species (**Figure 4**). However, this would also imply that porcelaneous, and high-Mg hyaline species that have the same D_{Mg} as high-Mg porcelaneous species (like *H. depressa*), should have a similar D_{Mn}. However, hyaline species have lower calcite Mn/Ca values compared to porcelaneous species, even when looking at species with similar Mg content, for instance *H. depressa* ($D_{Mg} \times 10^3 = 26.7$, $D_{Mn} = 1.9$) compared to *S. marginalis* ($D_{Mg} \times 10^3 = 26.6$, $D_{Mn} = 13.2$), which incorporates ~7 times more Mn while Mg content is similar (**Figure 4**). This suggests there is an additional process, probably fundamentally related to calcification of either hyaline or porcelaneous shells, which respectively decreases or increases the Mn/Ca of the precipitated calcite.

Potential Constrains for Mn/Ca As a (Paleo-) Oxygenation Proxy

In this study we observed that partitioning of Mn is species-specific and that Mn/Ca is positively correlated with pCO₂ (**Figure 1**) and/or negatively correlated with pH, [CO₃²⁻], Ω (**Supplementary Figure S1**). Although it is complicated to incisively explain this empirical relation with a single process, these observations have to be taken into account when applying Mn/Ca to field or (sub) geological samples as a proxy for oxygenation (Groeneveld and Filipsson, 2013; Ní Fhlaithearta et al., 2018; Petersen et al., 2018; Guo et al., 2019). Calibrations of the Mn/Ca oxygenation proxy for foraminifera require quantifying the direct impact of carbonate parameters on the proxy sensitivity, especially since covariation between pCO₂ and oxygenation can occur in benthic environments. However, we expect that for benthic species the impact of differences in carbonate chemistry on foraminiferal Mn/Ca is limited compared to the effect of oxygen-induced changes in Mn²⁺ and subsequently foraminiferal Mn/Ca, due to the low sensitivity observed in this study (**Figure 1**). Further studies are needed to decouple the effect of both environmental parameters, like obtaining sensitivity of Mn/Ca of larger benthic species to changes in O₂/seawater [Mn²⁺]. Furthermore, for calibration studies, in the water column, parameters of the carbonate chemistry will behave similar to this culture experiments, but in the sediment, characterized by high alkalinity, changes in carbonate chemistry might be buffered, and fluctuations in e.g., pH could therefore become negligible. More importantly, our observations of major differences in Mn incorporation between hyaline, both low and high Mg species, and porcelaneous species (**Figure 4**) is crucial to take into account for calibration and application of a potential O₂ proxy. Reconstructing oxygen concentration requires species-specific calibrations for Mn/Ca as well as insight into factors potentially affecting Mn speciation.

CONCLUSIONS

Manganese incorporation in two larger benthic foraminifera, *A. gibbosa* and *S. marginalis* is shown to be affected by seawater carbonate chemistry. Average chamber addition rate in the studied species is not impacted by the range in carbonate chemistry studies in this short-term culture experiment. We show that for both species, grown in controlled conditions, shell Mn/Ca increases with pCO₂ and hypothesize that this might not (only) be caused by changes of growth or precipitation rate or adsorption of Mn to the shell surface, but is likely impacted by changes in Mn speciation in seawater. Furthermore, in contrast to porcelaneous species, Mg and Mn incorporation in hyaline species seems to be correlated on specimen and species level, suggesting that the transport of both ions is somehow coupled during foraminiferal calcification. The high species-specific differences in partitioning of Mn calls for species-specific calibrations for Mn/Ca with oxygen content for proper application of the foraminiferal based Mn-oxygen proxy.

DATA AVAILABILITY STATEMENT

The raw data supporting the conclusions of this article will be made available by the authors, without undue reservation. LA-ICP-MS data is provided in the **Supplementary Material**.

AUTHOR CONTRIBUTIONS

IvD, LdN, and GJR designed the experiment, IvD performed the experiment and measurements. IvD, LdN, CB, and GJR discussed the data and wrote the manuscript. All authors contributed to data interpretation and writing of the final manuscript.

FUNDING

ACKNOWLEDGMENTS

from the tropical aquarium. Great thanks to Wim Boer for support with LA-Q-ICP-MS measurements and we would like to thank Kirsten Kooijman (Algae culturing), Patrick Laan (SF-ICP-MS), Karel Bakker (DIC) and Jan-Berend Stuut (SEM) for analysis and lab support.

SUPPLEMENTARY MATERIAL

The Supplementary Material for this article can be found online at: https://www.frontiersin.org/articles/10.3389/feart.2020.567701/full#supplementary-material

REFERENCES

Barker, S., Cacho, I., Benway, H., and Tachikawa, K. (2005). Planktonic foraminiferal Mg/Ca as a proxy for past oceanic temperatures: a methodological overview and data compilation for the Last Glacial Maximum. *Quat. Sci. Rev.* 24, 821–834. doi:10.1016/j.quascirev.2004.07.016

Barker, S., Greaves, M., and Elderfield, H. (2003). A study of cleaning procedures used for foraminiferal Mg/Ca paleothermometry. *Geochem. Geophys. Geosyst.* 4, 1–8. doi:10.1029/2003gc000559

Barras, C., Mouret, A., Nardelli, M. P., Metzger, E., Petersen, J., La, C., et al. (2018). Experimental calibration of manganese incorporation in foraminiferal calcite. *Geochim. Cosmochim. Acta.* 237, 49–64. doi:10.1016/j.gca.2018.06.009

Bé, A. W. H., Hemleben, C., Anderson, O. R., Spindler, M., and Be, A. W. H. (1979). Chamber formation in planktonic foraminifera. *Micropaleontology.* 25, 294–307. doi:10.2307/1485304

Bentov, S., Brownlee, C., and Erez, J. (2009). The role of seawater endocytosis in the biomineralization process in calcareous foraminifera. *Proc. Natl. Acad. Sci. U. S. A.* 106, 21500–21504. doi:10.1073/pnas.0906636106

Bentov, S., and Erez, J. (2006). Impact of biomineralization processes on the Mg content of foraminiferal shells: a biological perspective. *Geochem. Geophys. Geosyst.* 7, 319. doi:10.1029/2005gc001015

de Nooijer, L. J., Spero, H. J., Erez, J., Bijma, J., and Reichart, G. J. (2014). Biomineralization in perforate foraminifera. *Earth Sci. Rev.* 135, 48–58. doi:10.1016/j.earscirev.2014.03.013

de Nooijer, L. J., Toyofuku, T., and Kitazato, H. (2009a). Foraminifera promote calcification by elevating their intracellular pH. *Proc. Natl. Acad. Sci. U.S.A.* 106, 15374–15378. doi:10.1073/pnas.0904306106

de Nooijer, L. J., Langer, G., Nehrke, G., and Bijma, J. (2009b). Physiological controls on seawater uptake and calcification in the benthic foraminifer Ammonia tepida. *Biogeosciences.* 6, 2669–2675.

Doo, S. S., Fujita, K., Byrne, M., and Uthicke, S. (2014). Fate of calcifying tropical symbiont-bearing large benthic foraminifera: living sands in a changing ocean. *Biol. Bull.* 226, 169–186. doi:10.1086/bblv226n3p169

Elderfield, H., Bertram, C., and Erez, J. (1996). A biomineralization model for the incorporation of trace elements into foraminiferal calcium carbonate. *Earth Planet. Sci. Lett.* 142, 409–423. doi:10.1016/0012-821x(96)00105-7

Erez, J. (2003). The source of ions for biomineralization in foraminifera and their implications for paleoceanographic proxies. *Rev. Mineral. Geochem.* 54, 115–150. doi:10.2113/0540115

Ernst, S., Janse, M., Renema, W., Kouwenhoven, T., Goudeau, M.-L., and Reichart, G.-J. (2011). Benthic foraminifera in a large Indo-Pacific coral reef aquarium. *J. Foraminifer. Res.* 41, 101–113. doi:10.2113/gsjfr.41.2.101

Evans, D., Erez, J., Oron, S., and Müller, W. (2015). Mg/Ca-temperature and seawater-test chemistry relationships in the shallow-dwelling large benthic foraminifera Operculina ammonoides. *Geochim. Cosmochim. Acta.* 148, 325–342. doi:10.1016/j.gca.2014.09.039

Evans, D., Müller, W., and Erez, J. (2018). Assessing foraminifera biomineralisation models through trace element data of cultures under variable seawater chemistry. *Geochim. Cosmochim. Acta.* 236, 198–217. doi:10.1016/j.gca.2018.02.048

Foster, G. L., and Rae, J. W. B. (2016). Reconstructing ocean pH with boron isotopes in foraminifera. *Ann. Rev. Earth Planet. Sci.* 44, 207–237. doi:10.1146/annurev-earth-060115-012226

Glas, M. S., Fabricius, K. E., de Beer, D., and Uthicke, S. (2012a). The O^2, pH and Ca^{2+} microenvironment of benthic foraminifera in a high CO_2 world. *PLoS ONE.* 7, e50010. doi:10.1371/journal.pone.0050010

Glas, M. S., Langer, G., and Keul, N. (2012b). Calcification acidifies the microenvironment of a benthic foraminifer (Ammonia sp.). *J. Exp. Mar. Biol. Ecol.* 424–425, 53–58. doi:10.1016/j.jembe.2012.05.006

Groeneveld, J., and Filipsson, H. L. (2013). Mg/Ca and Mn/Ca ratios in benthic foraminifera: the potential to reconstruct past variations in temperature and hypoxia in shelf regions. *Biogeosciences.* 10, 5125–5138. doi:10.5194/bg-10-5125-2013

Gonçalves, P., Meireles, S., Neves, P., and Vale, M. (1999). Ionic selectivity of the Ca2+/H+ antiport in synaptic vesicles of sheep brain cortex. *Mol. Brain Res.* 67 (2), 283–291. doi:10.1016/S0169-328X(99)00081-9

Guillong, M., Meier, D. L., Allan, M. M., Heinrich, C. A., and Yardley, B. W. (2008). SILLS: a MATLAB-based program for the reduction of laser ablation ICP-MS data of homogeneous materials and inclusions. *Miner. Assoc. Canada Short Course Ser.* 40, 328–333.

Guo, X., Xu, B., Burnett, W. C., Yu, Z., Yang, S., Huang, X., et al. (2019). A potential proxy for seasonal hypoxia: LA-ICP-MS Mn/Ca ratios in benthic foraminifera from the Yangtze River Estuary. *Geochim. Cosmochim. Acta.* 245, 290–303. doi:10.1016/j.gca.2018.11.007

Hemleben, C. H., Anderson, O. R., Berthold, W., and Spindler, M. (1986). "Calcification and chamber formation in Foraminifera-a brief overview," in *Biomineralization in lower plants and animals.* Editors B. S. Leadbeater and R. Riding (Oxford, UK: Clarendon Press), 237–249.

Jacob, D. E., Wirth, R., Agbaje, O. B. A., Branson, O., and Eggins, S. M. (2017). Planktic foraminifera form their shells via metastable carbonate phases. *Nat. Commun.* 8, 1265. doi:10.1038/s41467-017-00955-0

Keul, N., Langer, G., de Nooijer, L. J., and Bijma, J. (2013). Effect of ocean acidification on the benthic foraminifera. *Biogeosciences* 10, 6185–6198. doi:10.5194/bg-10-6185-2013

Keul, N., Langer, G., Thoms, S., de Nooijer, L. J., Reichart, G. J., and Bijma, J. (2017). Exploring foraminiferal Sr/Ca as a new carbonate system proxy. *Geochem. Cosmochim. Acta.* 202, 374–386. doi:10.1016/j.gca.2016.11.022

Koho, K. A., de Nooijer, L. J., and Reichart, G. J. (2015). Combining benthic foraminiferal ecology and shell Mn/Ca to deconvolve past bottom water oxygenation and paleoproductivity. *Geochem. Cosmochim. Acta.* 165, 294–306. doi:10.1016/j.gca.2015.06.003

Kroeker, K. J., Kordas, R. L., Crim, R., Hendriks, I. E., Ramajo, L., Singh, G. S., et al. (2013). Impacts of ocean acidification on marine organisms: quantifying sensitivities and interaction with warming. *Glob. Chang. Biol.* 19, 1884–1896. doi:10.1111/gcb.12179

Lear, C. H., Elderfield, H., and Wilson, P. A. (2000). Cenozoic deep-Sea temperatures and global ice volumes from Mg/Ca in benthic foraminiferal calcite. *Science* 287, 269–272. doi:10.1126/science.287.5451.269

Lee, J. J., Morales, J., Symons, A., and Hallock, P. (1995). Diatom symbionts in larger foraminifera from Caribbean hosts. *Mar. Micropaleontol.* 26, 99–105. doi:10.1016/0377-8398(95)00004-6

Lorens, R. B. (1981). Sr, Cd, Mn and Co distribution coefficients in calcite as a function of calcite precipitation rate. *Geochem. Cosmochim. Acta.* 45, 553–561. doi:10.1016/0016-7037(81)90188-5

Müller-Merz, E., and Lee, J. J. (1976). Symbiosis in the larger foraminiferan Sorites marginalis (with notes on Archaias spp.). *J. Protozool.* 23, 390–396. doi:10.1111/j.1550-7408.1976.tb03793.x

Mavromatis, V., Gautier, Q., Bosc, O., and Schott, J. (2013). Kinetics of Mg partition and Mg stable isotope fractionation during its incorporation in calcite. *Geochem. Cosmochim. Acta.* 114, 188–203. doi:10.1016/j.gca.2013.03.024

McKay, C. L., Groeneveld, J., Filipsson, H. L., Gallego-Torres, D., Whitehouse, M. J., Toyofuku, T., et al. (2015). A comparison of benthic foraminiferal Mn/Ca and sedimentary Mn/Al as proxies of relative bottom-water oxygenation in the low-latitude NE Atlantic upwelling system. *Biogeosciences* 12, 5415–5428. doi:10.5194/bg-12-5415-2015

Mewes, A., Langer, G., Reichart, G. J., de Nooijer, L. J., Nehrke, G., and Bijma, J. (2015). The impact of Mg contents on Sr partitioning in benthic foraminifers. *Chem. Geol.* 412, 92–98. doi:10.1016/j.chemgeo.2015.06.026

Mezger, E. M., de Nooijer, L. J., Boer, W., Brummer, G. J. A., and Reichart, G. J. (2016). Salinity controls on Na incorporation in Red Sea planktonic foraminifera. *Paleoceanography* 31, 1562–1582. doi:10.1002/2016pa003052

Middelburg, J. J., De Lange, G. J., and van Der Weijden, C. H. (1987). Manganese solubility control in marine pore waters. *Geochem. Cosmochim. Acta.* 51, 759–763. doi:10.1016/0016-7037(87)90086-x

Mucci, A. (1987). Influence of temperature on the composition of magnesian calcite overgrowths precipitated from seawater. *Geochem. Cosmochim. Acta.* 51, 1977–1984. doi:10.1016/0016-7037(87)90186-4

Mucci, A., and Morse, J. W. (1983). The incorporation of Mg^{2+} and Sr^{2+} into calcite overgrowths: influences of growth rate and solution composition. *Geochem. Cosmochim. Acta.* 47, 217–233. doi:10.1016/0016-7037(83)90135-7

Nehrke, G., Keul, N., Langer, G., de Nooijer, L. J., Bijma, J., and Meibom, A. (2013). A new model for biomineralization and trace - element signatures of Foraminifera tests. *Biogeosciences* 10, 6759–6767. doi:10.5194/bg-10-6759-2013

Ní Fhlaithearta, S., Fontanier, C., Jorissen, F., Mouret, A., Dueñas-Bohórquez, A., and Anschutz, P. (2018). Manganese incorporation in living (stained) benthic foraminiferal shells: a bathymetric and in-sediment study in the Gulf of Lions (NW Mediterranean). *Biogeosciences.* 15, 6315–6328. doi:10.5194/bg-15-6315-2018

Nürnberg, D., Bijma, J., and Hemleben, C. (1996). Assessing the reliability of magnesium in foraminiferal calcite as a proxy for water mass temperatures. *Geochem. Cosmochim. Acta.* 60, 803–814. doi:10.1016/0016-7037(95)00446-7

Okai, T., Suzuki, A., Kawahata, H., Terashima, S., and Imai, N. (2002). Preparation of a new geological survey of Japan geochemical reference material: coral JCp-1. *Geostand. Newsl.* 26, 95–99. doi:10.1111/j.1751-908x.2002.tb00627.x

Orr, J. C., Fabry, V. J., Aumont, O., Bopp, L., Doney, S. C., Feely, R. A., et al. (2005). Anthropogenic ocean acidification over the twenty-first century and its impact on calcifying organisms. *Nature* 437, 681–686. doi:10.1038/nature04095

Pagani, M., Lemarchand, D., Spivack, A., and Gaillardet, J. (2005). A critical evaluation of the boron isotope-pH proxy: the accuracy of ancient ocean pH estimates. *Geochem. Cosmochim. Acta.* 69, 953–961. doi:10.1016/j.gca.2004.07.029

Parkhurst, D. L., and Appelo, C. (1999). *User's guide to PHREEQC (version 2): a computer program for speciation, batch-reaction, one-dimensional transport, and inverse geochemical calculations.* Denver, CO: US Geological Survey.

Petersen, J., Barras, C., Bézos, A., La, C., de Nooijer, L. J., Meysman, F. J. R., et al. (2018). Mn/Ca intra- and inter-test variability in the benthic foraminifer *Ammonia tepida. Biogeosciences* 15, 331–348. doi:10.5194/bg-15-331-2018

Prazeres, M., Uthicke, S., and Pandolfi, J. M. (2015). Ocean acidification induces biochemical and morphological changes in the calcification process of large benthic foraminifera. *Proc. R. Soc. Lond. B Biol. Sci.* 282. doi:10.1098/rspb.2014.2782

Reichart, G.-J., Jorissen, F., Anschutz, P., and Mason, P. R. (2003). Single foraminiferal test chemistry records the marine environment. *Geology* 31, 355–358. doi:10.1130/0091-7613(2003)031<0355:sftcrt>2.0.co;2

Ries, J. B., Cohen, A. L., and McCorkle, D. C. (2009). Marine calcifiers exhibit mixed responses to CO$_2$-induced ocean acidification. *Geology* 37, 1131–1134. doi:10.1130/g30210a.1

Sanyal, A., Hemming, N. G., Broecker, W. S., Lea, D. W., Spero, H. J., and Hanson, G. N. (1996). Oceanic pH control on the boron isotopic composition of foraminifera: evidence from culture experiments. *Paleoceanography* 11, 513–517. doi:10.1029/96pa01858

Toyofuku, T., Matsuo, M. Y., de Nooijer, L. J., Nagai, Y., Kawada, S., Fujita, K., et al. (2017). Proton pumping accompanies calcification in foraminifera. *Nat. Commun.* 8, 14145. doi:10.1038/ncomms14145

Toyofuku, T., Suzuki, M., Suga, H., Sakai, S., Suzuki, A., Ishikawa, T., et al. (2011). Mg/Ca and δ^{18}O in the brackish shallow-water benthic foraminifer *Ammonia 'beccarii.' Mar. Micropaleontol.* 78, 113–120. doi:10.1016/j.marmicro.2010.11.003

Tribovillard, N., Algeo, T. J., Lyons, T., and Riboulleau, A. (2006). Trace metals as paleoredox and paleoproductivity proxies: an update. *Chem. Geol.* 232, 12–32. doi:10.1016/j.chemgeo.2006.02.012

Van Dijk, I., Barras, C., de Nooijer, L. J., Mouret, A., Geerken, E., Oron, S., et al. (2019a). Coupled calcium and inorganic carbon uptake suggested by magnesium and sulfur incorporation in foraminiferal calcite. *Biogeosciences* 16, 2115–2130. doi:10.5194/bg-16-2115-2019

Van Dijk, I., de Nooijer, L. J., Boer, W., and Reichart, G. J. (2017a). Sulfur in foraminiferal calcite as a potential proxy for seawater carbonate ion concentration. *Earth Planet Sci. Lett.* 470, 64–72. doi:10.1016/j.epsl.2017.04.031

Van Dijk, I., de Nooijer, L. J., and Reichart, G. J. (2017b). Trends in element incorporation in hyaline and porcelaneous foraminifera as a function of pCO$_2$. *Biogeosciences* 14, 497–510. doi:10.5194/bg-14-497-2017

Van Dijk, I., de Nooijer, L. J., Wolthers, M., and Reichart, G. J. (2017c). Impacts of pH and [CO$_3^{2-}$] on the incorporation of Zn in foraminiferal calcite. *Geochem. Cosmochim. Acta.* 197, 263–277. doi:10.1016/j.gca.2016.10.031

Van Dijk, I., Mouret, A., Cotte, M., Le Houedec, S., Oron, S., Reichart, G.-J., et al. (2019b). Chemical heterogeneity of Mg, Mn, Na, S, and Sr in benthic foraminiferal calcite. *Front. Earth Sci.* 7, 281. doi:10.3389/feart.2019.00281

Vogel, N., and Uthicke, S. (2012). Calcification and photobiology in symbiont-bearing benthic foraminifera and responses to a high CO$_2$ environment. *J. Exp. Mar. Biol. Ecol.* 424–425, 15–24. doi:10.1016/j.jembe.2012.05.008

Webb, A. E., van Heuven, S. M. A. C., de Bakker, D. M., van Duyl, F. C., Reichart, G.-J., and de Nooijer, L. J. (2017). Combined effects of experimental acidification and eutrophication on reef sponge bioerosion rates. *Front. Mar. Sci.* 4, 313–315. doi:10.3389/fmars.2017.00311

Zachara, J. M., Cowan, C. E., and Resch, C. T. (1991). Sorption of divalent metals on calcite. *Geochem. Cosmochim. Acta.* 55, 1549–1562. doi:10.1016/0016-7037(91)90127-q